Modeling and Controller Design of Hydraulic Rotorcraft Aerial Manipulator

Lin Tianyu[1,2], Li Yongzhe[3], Qi Juntong[1], Meng Xiangdong[1], Han Jianda[1]

1. State Key Laboratory of Robotics, Shenyang Institute of Automation, Chinese Academy of Sciences, Shenyang 110016

E-mail: qijt@sia.cn, xdmeng09@163.com, jdhan@sia.cn

2. Shenyang Ligong University, Shenyang 110159

E-mail: razorwoods@126.com

3. Northeastern University, Shenyang 110819

Abstract: Traditional Rotary-wing Unmanned Aerial Vehicles (R-UAV) are mostly utilized to conduct surveillance. Installing a mechanical manipulator on R-UAV will result a Rotorcraft Aerial Manipulator (RAM) system. A RAM system enlarges the R-UAV's application scope. The RAM system proposed by this research is composed of R-UAV and a miniature hydraulic manipulator. With the combined merits of the two systems, this RAM system has enhanced flexibility and is capable of fulfilling more tasks. The hovering mode dynamics model of the RAM is established referring to the working characteristics of the hydraulic manipulator. An LQR controller is used to control the planar motion of the hydraulic manipulator. The motion of the manipulator will exert coupled force and moment influence on the RAM system. This coupled influence is taken as a disturbance to the R-UAV system which is restrained by a robust controller. Finally, through simulation, the effectiveness of the established dynamics model and the proposed control strategy is verified.

Key Words: RAM, Hydraulic manipulator, Modeling, LQR controller, Robust controller

1 INTRODUCTION

Mobile operational ground robot systems (a combination of ground mobile robot and mechanical arm), are utilized in disaster relief ,anti-terrorism and anti-riot occasions etc. They have been fully verified as well as widely recognized. The idea of combining the operational ability of mechanical arms and the mobility of mobile robots thus expanding the scope of application of robots is highly attractive.

With the extension of robots' applications, people are more eager to witness that flying robots can exert active influences on the environment. Installing an operating manipulator mechanism onto flying robot platform thus endowing the robot active operation capability in complex 3D working environment is highly practically significant. The design idea of most flying robots is to avoid contact with the environment. Yet RUAVs have the characteristics of hovering and high mobility, and can replace humans in acquiring information in risky and hazardous environments. For this reason, people are hoping that the RUAVs can conduct maneuvers that effectively contact the environment. To realize this hope, the research of the contact between RUAV and its environment has already become a hotspot, and has attracted extensive attention in the flying robot domain.

The concept of combining a RUAV and a manipulator has been preliminarily validated by several research institutes. The Yale Aerial Manipulator [1] has a compliant gripper which can grasp objects while landed or hovering. Here, the system stable area was evaluated with reference to the position of the payload relative to the system's center of gravity (CG). The University of Pennsylvania's research [2] adopted the method of parameter estimation, and estimated the uncertain parameters of RAM when grasping payloads. The RAM system from DLR [3] is loaded with a 7-DOF industrial manipulator and is able to grasp long sticks on the ground. Here, the control issues involving the CG change of the RAM system when grasping had been studied. In addition, there are some other researches on multi-rotor aircraft mounted with a manipulator which can grasp lightweight objects [3-5].

The examples mentioned above all use electric motors to drive the manipulators, and all mount the manipulator on the RUAV to grasp light weight or fixed shape objects. Yet in reality, many demands cannot be met by simple grasping maneuver, such as the maintenance of high voltage power transmission lines. The severing off operation of damaged power lines requires great force and torque. This operation requires the end-effector to be very powerful and finish the cutting off operation in a short time. However, none of the aforementioned papers discussed such an operation. Also none of the end-effectors mentioned in those papers has adequate power to perform this kind of operation. If an electric motor is chosen to drive the end-effector, the gear box will become a heavy burden for the RUAV and the vibration of the motor and the gear box will induce extra disturbance.

To solve this problem, a novel RUAV mobile operating system is proposed which is composed of an RUAV and a multiple degrees of freedom (DOF) miniature hydraulic manipulator shown in Figure 1. Hydraulic system is chosen because it has many advantages compared to electric or pneumatic systems. Power in the hydraulic system is

---

This work is supported by National Natural Science Foundation of China (Project 61433016 and 61273025)

transmitted through the continuous flow of the hydraulic oil making the transmission is very smooth and shock absorbent causing little vibration. When the output power is the same, hydraulic transmission's volume and weight are much lower giving it less inertia. More importantly, large force and torque are easily achievable for hydraulic transmission and the mechanical structure is simplified, thus reducing the number of components and fault rate.

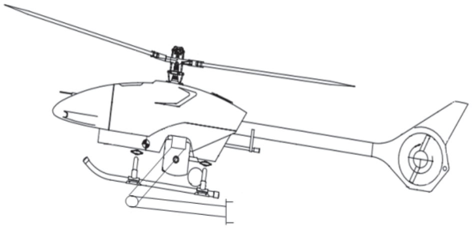

Fig.1 Rotorcraft aerial manipulator system

Fig. 2 SIA RUAV transporting a barrel

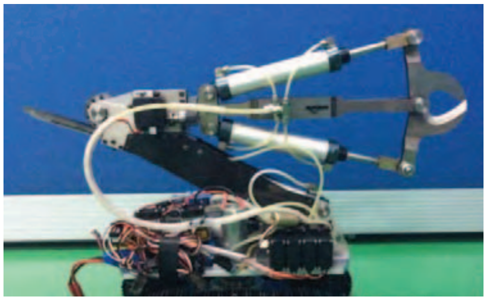

Fig.3 SIA 4-DOF miniature hydraulic manipulator

For these reasons, installing a miniature hydraulic manipulator onto an RUAV (Figure 2) to obtain a whole new hydraulic RAM system will enhance RUAV's capability to fulfill more tasks. To date, we have already designed and produced the first prototype of the hydraulic manipulator (Figure 3). The dynamics modeling and controller design are ongoing and will facilitate the simulation of the model. The relative dynamics between the RUAV and the hydraulic manipulator is treated as internal disturbance which is modeled via dynamic analysis. The contents of this paper are as follows. Firstly, according to Newton-Euler equations and the aerial dynamic characteristics of the RUAV, the dynamic model of the hydraulic RAM system is established. Then, in the hovering mode of the RUAV, an LQR controller is utilized to control the hydraulic manipulator; at which time, the manipulator's movement is regarded as a disturbance to the RUAV and a robust controller is employed to adjust the RUAV's pose. Finally, the end-effector's arc trace of the hydraulic manipulator is simulated, and through simulation, the performance of RAM's robust controller is evaluated.

2 MODELING OF THE HYDRAULIC RAM SYSTEM

To control the hydraulic RAM system, the hydraulic RAM system's dynamics model needs to be studied and analyzed [6-7]. In practice, the manipulator's movements mostly occur in the hovering mode of the RUAV. Based on this fact, the dynamics modeling of the designed hydraulic manipulator can use traditional robot manipulator theory. For the dynamics model of the RAM system, i.e. the 6-DOF rigid body's dynamic expression of the RAM, the combination of different sourced force and moment can be taken in to account.

2.1 Coordinates of the Manipulator's Links

The fuselage of the RUAV is regarded as the base of the hydraulic manipulator, so it is link 0. The revolving chassis of the 4-DOF manipulator is link 1 and is connected to link 0 through joint 1. Link 2 and link 1 are connected by joint 2 and so on until the last link. The coordinate systems here are similar to those from Denavit-Hartenberg (D-H) method. The Z_i axis of coordinates {i} is collinear with joint axis i, its pointing is arbitrary. The X_i axis of coordinates {i} is collinear with the joint axes' common normal and points from joint i to joint i+1. The Y axes are determined by the right-hand rule. The D-H coordinates of the abstract manipulator model are shown in Figure 4.

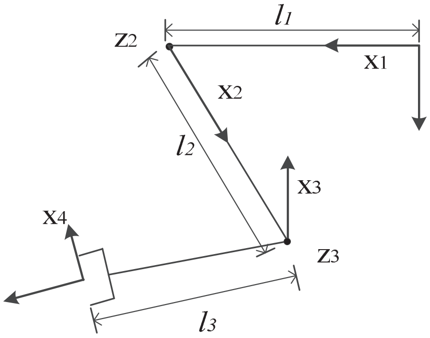

Fig.4 Coordinates of abstract manipulator model

Using the method above, measure and substitute each links' parameters into corresponding transformation matrices, and the transformation matrices between adjacent links' coordinates are yielded. The 4-DOF manipulator linkage parameters are shown in Table 1.

Tab.1 4-DOF manipulator linkage parameters

i	a_{i-1}	α_{i-1}	d_i	θ_i
1	0	0°	0	θ_1
2	l_1	-90°	0	θ_2
3	l_2	0°	0	θ_3
4	0°	90°	l_3	θ_4

D-H parameters method is used to describe the relative location between adjacent links and finally obtain the transformation relationships between the adjacent coordinates. Through a sequenced rotation and translation, we can obtain the transformation matrix between adjacent coordinates:

$$
{}^{i-1}_{\;\;i}T = R_X(\alpha_{i-1})D_X(a_{i-1})R_Z(\theta_i)D_Z(d_i)\,\mathrm{T}
$$

$$
= \begin{bmatrix} \cos\theta_i & -\sin\theta_i & 0 & a_{i-1} \\ \sin\theta_i\cos\alpha_{i-1} & \cos\theta_i\cos\alpha_{i-1} & -\sin\alpha_{i-1} & -\sin\alpha_{i-1}d_{i-1} \\ \sin\theta_i\sin\alpha_{i-1} & \cos\theta_i\sin\alpha_{i-1} & \cos\alpha_{i-1} & \cos\alpha_{i-1}d_{i-1} \\ 0 & 0 & 0 & 1 \end{bmatrix} \quad (1)
$$

So the transformation matrix from the end to the base coordinates is:

$$
{}^0_4T = \begin{bmatrix} \mathrm{c}\theta_1\mathrm{c}\theta_{23}\mathrm{c}\theta_4 - \mathrm{s}\theta_1\mathrm{s}\theta_4 & -\mathrm{c}\theta_1\mathrm{c}\theta_{23}\mathrm{s}\theta_4 - \mathrm{s}\theta_1\mathrm{c}\theta_4 & \mathrm{c}\theta_1\mathrm{s}\theta_{23} & r_{14} \\ \mathrm{s}\theta_1\mathrm{c}\theta_{23}\mathrm{c}\theta_4 + \mathrm{c}\theta_1\mathrm{s}\theta_4 & -\mathrm{s}\theta_1\mathrm{c}\theta_{23}\mathrm{s}\theta_4 + \mathrm{c}\theta_1\mathrm{c}\theta_4 & \mathrm{s}\theta_1\mathrm{s}\theta_{23} & r_{24} \\ -\mathrm{s}\theta_{23}\mathrm{c}\theta_4 & \mathrm{s}\theta_{23}\mathrm{s}\theta_4 & \mathrm{c}\theta_{23} & r_{34} \\ 0 & 0 & 0 & 1 \end{bmatrix} \quad (2)
$$

$$
r_{14} = l_1\,\mathrm{c}\,\theta_1 + l_2\,\mathrm{c}\,\theta_1\,\mathrm{c}\,\theta_2 + l_3\,\mathrm{c}\,\theta_1\,\mathrm{s}\,\theta_{23},\quad r_{34} = -l_2\,\mathrm{s}\,\theta_2 + l_3\,\mathrm{c}\,\theta_{23},
$$

$$
r_{24} = l_1\,\mathrm{s}\,\theta_1 + l_2\,\mathrm{s}\,\theta_1\,\mathrm{c}\,\theta_2 + l_3\,\mathrm{s}\,\theta_1\,\mathrm{s}\,\theta_{23}
$$

The chassis of the 4-DOF manipulator does not need to rotate, so $\theta_1 = 0, \mathrm{c}\,\theta_1 = 1, \mathrm{s}\,\theta_1 = 0$, and the end hydraulic scissors' azimuth does not need to change. So $\theta_4 = 0, \mathrm{c}\,\theta_4 = 1, \mathrm{s}\,\theta_4 = 0$, thus matrix (2) is reduced to:

$$
{}^0_4T = \begin{bmatrix} \mathrm{c}\,\theta_{23} & 0 & \mathrm{s}\,\theta_{23} & l_1 + l_2\,\mathrm{c}\,\theta_2 + l_3\,\mathrm{s}\,\theta_{23} \\ 0 & 1 & 0 & 0 \\ -\mathrm{s}\,\theta_{23} & 0 & \mathrm{c}\,\theta_{23} & -l_2\,\mathrm{s}\,\theta_2 + l_3\,\mathrm{c}\,\theta_{23} \\ 0 & 0 & 0 & 1 \end{bmatrix} \quad (3)
$$

2.2 Modeling of the RAM System

Traditional RUAV's models do not account for the influence from the manipulator to the fuselage. So RUAV's model [8-10] needs to be improved. The influence from the manipulator to the fuselage is added to meet the control requirements of the RAM. Below, the RUAV's model is given, and the influence from the manipulator to the fuselage is added based on the model.

Normally, RUAV model is set on its fuselage coordinate, i.e. X axis points to the head of the helicopter, Y axis points to the right flank and Z axis points to the bottom. These three axes satisfy the right hand rule. In this paper's research, the RAM's position and attitude are to be controlled, yet position and attitude are defined in the world coordinate system. The two coordinate systems can be converted to each other via a rotation matrix. The rotation matrix from fuselage coordinates (body frame) to world coordinates is:

$$
R_{b\to W} = \begin{bmatrix} \mathrm{c}\phi\mathrm{c}\psi & \mathrm{s}\phi\mathrm{s}\theta\mathrm{c}\psi - \mathrm{c}\phi\mathrm{s}\psi & \mathrm{c}\phi\mathrm{s}\theta\mathrm{c}\psi + \mathrm{s}\phi\mathrm{s}\psi \\ \mathrm{c}\theta\mathrm{s}\psi & \mathrm{s}\phi\mathrm{s}\theta\mathrm{s}\psi + \mathrm{c}\phi\mathrm{c}\psi & \mathrm{c}\phi\mathrm{s}\theta\mathrm{s}\psi - \mathrm{s}\phi\mathrm{c}\psi \\ -\mathrm{s}\theta & \mathrm{s}\phi\mathrm{c}\theta & \mathrm{c}\phi\mathrm{c}\theta \end{bmatrix} \quad (4)
$$

Where $[\phi,\theta,\psi]$ represents the RAM's roll, pitch and yaw angles. The fuselage's speed and position in the world coordinates can be expressed as:

$$
\dot{P}_W = R_{b\to W}V_b \quad (5)
$$

Where $P = [x, y, z]$ represent position, $V_b = [u_b, v_b, w_b]$ represent RUAV's forward, lateral and vertical speed. Subscript W indicates that the variables are defined in the world coordinates, subscript b indicates that the variables are defined in the fuselage coordinates.

Next, the model of the RUAV in its fuselage coordinates will be briefly analyzed. Firstly, we consider rotation:

$$
\begin{bmatrix} \dot{\phi} \\ \dot{\theta} \\ \dot{\psi} \end{bmatrix} = \begin{bmatrix} 1 & \sin\phi\tan\theta & \cos\phi\tan\theta \\ 0 & \cos\phi & -\sin\phi \\ 0 & \sin\phi/\cos\theta & \cos\phi/\cos\theta \end{bmatrix} \begin{bmatrix} p \\ q \\ r \end{bmatrix} \quad (6)
$$

Where $\omega_b = [p, q, r]$ are the RUAV's roll, pitch and yaw angular velocities. The 6-DOF rigid body's dynamics can be described by Newton-Euler equations:

$$
\begin{aligned} \dot{V}_b &= -\omega_b \times V_b + \frac{F_b}{m} + \frac{F_g}{m} \\ \dot{\omega}_b &= I_b^{-1}\left[M_b - \omega_b \times (I_b\omega_b)\right] \end{aligned} \quad (7)
$$

Where F_b is aerodynamic force vector, M_b is aerodynamic moment vector, F_g is gravity vector, I_b is rotary inertia, m is the weight of the RAM. Normally, aerodynamic force and moment can be expressed using the nonlinear functions below:

$$
\begin{aligned} F_b &= f_f(a_{1s}, b_{1s}, \delta_{col}, \delta_{ped}) \\ M_b &= f_m(a_{1s}, b_{1s}, \delta_{col}, \delta_{ped}) \end{aligned} \quad (8)
$$

Where, f_f, f_m are nonlinear functions, and can be obtained through aerodynamic analysis. a_{1s}, b_{1s} are longitudinal and transverse flapping angle of the main blade. δ_{col} is the pitch angle of the main blade, δ_{ped} is the pitch angle of the tail blade. Considering the flapping dynamics of the main blade:

$$
\begin{aligned} \dot{a}_{1s} &= -q - \frac{1}{}\frac{1}{\tau_{mr}}a_{1s} + A_{bs}b_{1s} + \frac{1}{\tau_{mr}}\delta_{lon} \\ \dot{b}_{1s} &= -p - \frac{1}{\tau_{mr}}b_{1s} + B_{as}a_{1s} + \frac{1}{\tau_{mr}}\delta_{lat} \end{aligned} \quad (9)
$$

Where τ_{mr} is the time constant of the main blade, A_{bs}, B_{as} are coupling coefficients, δ_{lon} and δ_{lat} are forward and lateral controlled quantity.

Equations (4)-(9) briefly described the general model of RUAV. Now, the influence from the manipulator to RUAV will be taken in to account, hence the model of hydraulic RAM system can be established. The manipulator and the RUAV's fuselage are connected by fixed joint so they can be taken as a rigid body. Its 6-DOF dynamics model can be described using the following Newton-Euler equations:

$$
\begin{aligned} \dot{V}_b &= -\omega_b \times V_b + \frac{F_b}{m'} + \frac{F'_g}{m'} + \frac{F_m}{m'} \\ \dot{\omega}_b &= I_b'^{-1}\left[M_b + M_m - \omega_b \times (I'_b\omega_b)\right] \end{aligned} \quad (10)
$$

Where F_m is the force vector exerted on the fuselage of the RUAV when the arm of the manipulator moves, M_m is the moment vector, F'_g is the gravity vector of RAM, I'_b is the rotary inertia, m' is the mass of the hydraulic RAM. F_m, M_m can be calculated by the following equations.

For ${}_{i}^{i-1}R, {}^{i-1}P_i$, their normal forms are:

$$ {}_{i}^{i-1}R = \begin{bmatrix} c\theta_i & -s\theta_i & 0 \\ s\theta_i c\alpha_{i-1} & c\theta_i c\alpha_{i-1} & -s\alpha_{i-1} \\ s\theta_i s\alpha_{i-1} & c\theta_i s\alpha_{i-1} & c\alpha_{i-1} \end{bmatrix}, \quad {}^{i-1}P_i = \begin{bmatrix} a_{i-1} \\ -s\alpha_{i-1} b_i \\ c\alpha_{i-1} b_i \end{bmatrix} \tag{11} $$

The force and moment of each link caused by the motion of the manipulator can be obtained by iteration from the end-effector link to the base link.

$$ \begin{aligned} {}^{i}f_i &= {}_{i+1}^{i}R\, {}^{i+1}f_{i+1} + {}^{i}F_i \\ {}^{i}m_i &= {}_{i+1}^{i}R\, {}^{i+1}m_{i+1} + {}^{i}P_{i+1} \times {}_{i+1}^{i}R\, {}^{i+1}f_{i+1} + {}^{i}P_{ci} \times {}^{i}F_i + {}^{i}m_i \end{aligned} \tag{12} $$

According to Newton’s third law, the force and moment exerted on the fuselage of the RAM are easily obtained:

$$ \begin{cases} F_m = -{}_{1}^{0}R\, {}^{1}f_1 \\ M_m = -{}_{1}^{0}R\, {}^{1}m_1 - {}^{0}P_1 \times {}_{1}^{0}R\, {}^{1}f_1 \end{cases} \tag{13} $$

3 CONTROL OF HYDRAULIC RAM SYSTEM

The hydraulic manipulator only operates in hovering mode of RAM, when the motion of the manipulator is controlled to complete tasks. The influence that the manipulator exerts to the fuselage of the RUAV is treated as disturbance and is restrained by robust controller.

3.1 Control of Hydraulic Manipulator System

From references [6-7], the open-loop transfer function of hydraulic actuator is

$$ G_m = \frac{0.001234s^2 + 12.34s + 0.987}{1.462\times10^{-9}s^6 + 3.038\times10^{-7}s^5 + 1.169\times10^{-4}s^4 + 0.0136s^3 + s^2} \tag{14} $$

Convert the above open-loop transfer function to state-space form:

$$ \begin{aligned} \dot{x}_m &= A_m x_m(t) + B_m u_m(t) \\ y_m &= C_m x_m(t) \end{aligned} \tag{15} $$

To realize the control of hydraulic actuator, a state feedback controller is designed:

$$ u_m(t) = K_m x_m(t) + K_{mr} ref_m \tag{16} $$

Where ref_m is reference input; K_m is feedback matrix, which ensures the stability of the system; K_{mr} is feed-forward matrix, which realizes the tracking of reference inputs. Feedback matrix K_m can be calculated through linear quadratic regulator (LQR) method, and the feed-forward matrix:

$$ K_{mr} = [C_m (A_m + B_m K_m)^{-1} B_m]^{+} \tag{17} $$

Where the symbol $[\cdot]^{+}$ indicates pseudo-inverse. However the state x_m of hydraulic actuator cannot be measured directly, so it needs to be observed by the following designed state observer:

$$ \dot{\hat{x}}_m = A_m \hat{x}_m(t) + B_m u_m(t) + L(y(t) - C\hat{x}_m(t)) \tag{18} $$

Where the state observer matrix L can be obtained through pole assignment method, thus the corresponding state feedback controller is:

$$ u_m(t) = K_m \hat{x}_m(t) + K_{mr} ref_m \tag{19} $$

3.2 Control of RUAV

To restrain the influence that the motion of the manipulator exerts on the RUAV, F_m and M_m are regarded as disturbances on the RUAV and are restrained through control algorithm.

Choose a stable state near the RUAV’s hovering point as the equilibrium point, and linearize the above model of the RAM which contains the influence of the manipulator, then the following linear model can be obtained:

$$ \begin{aligned} \dot{x}_p(t) &= A_p x_p(t) + B_p u(t) + E_p \omega_p(t) \\ y_p(t) &= C_1 x_p(t) \\ z_p(t) &= C_2 x_p(t) \end{aligned} \tag{20} $$

Where, $x_p = [u_b, v_b, w_b, \phi, \theta, \psi, p, q, r, a_{1s}, b_{1s}]$ are the system state vectors, $u = \left[\delta_{lon}, \delta_{lat}, \delta_{col}, \delta_{ped}\right]$ are control inputs, $y_p = [u_b, v_b, w_b, \phi, \theta, \psi, p, q, r]$ are the measured outputs of the system, $z_p = [u_b, v_b, w_b, \psi]$ are controllable system outputs, ω_p is disturbance. A_p, B_p, E_p, C_1, C_2 are constant matrices of appropriate dimensions.

To implement tracking control of the RUAV, the error vector $e(t) = \int ref - z(t)dt$ is defined, then the above function can be expressed as:

$$ \begin{aligned} \dot{x}_e(t) &= A_e x_e + B_e u(t) + E_e \omega_p(t) + R_e ref \\ y_p(t) &= C_{e1} x_e(t) \\ z_p(t) &= C_{e2} x_e(t) \end{aligned} \tag{21} $$

Where $x_e(t) = [x_p^T(t)\; e^T(t)]^T$, $A_e = \begin{bmatrix} A_p & 0 \\ -C_2 & 0 \end{bmatrix}$,

$B_e = \begin{bmatrix} B_p & 0 \end{bmatrix}^T$, $E_e = \begin{bmatrix} E_p & 0 \end{bmatrix}^T$, $R_e = [0 \quad I]^T$,

$C_{e1} = [C_1 \quad 0]$, $C_{e2} = [C_2 \quad 0]$.

Furthermore, let $E_r \omega(t) = E_e \omega_p(t) + R_e ref$, then

$$ \dot{x}_e(t) = A_e x_e + B_e u(t) + E_r \omega(t) \tag{22} $$

To minimize the influence of the disturbance on the system and guarantee a certain tracking accuracy, a controller needs to be designed to control the above system. Yet

a_{1s}, b_{1s} of the system state cannot be measured by sensors directly, thus the following dynamic output feedback controller is designed:

$$\begin{aligned}\dot{x}_c(t) &= A_c x_c(t) + B_c y_p(t)\\ u(t) &= C_c x_c(t) + D_c y_p(t)\end{aligned} \tag{23}$$

Where x_c is the state vector of the controller, it has the same dimensions with x_p , A_c, B_c, C_c, D_c are undetermined controller matrices, thus the closed-loop system can be expressed as:

$$\begin{aligned}\dot{x}(t) &= Ax(t) + E\omega(t)\\ z_p(t) &= Cx(t)\end{aligned} \tag{24}$$

Where $x(t) = [x_e^T(t)\ x_c^T(t)]^T$,

$$A = \begin{bmatrix} A_e + B_e D_c C_{e1} & B_e C_c \\ B_c C_{e1} & A_c \end{bmatrix},\ E = \begin{bmatrix} E_r \\ 0 \end{bmatrix},\ C = \begin{bmatrix} C_{e2} \\ 0 \end{bmatrix}^T$$

To minimize the influence that $\omega(t)$ exerts on the system, consider H_∞ criterion $\|e\|_2 = \|ref - z_p(t)\|_2 \le \gamma \|\omega\|_2$. According to reference [11], H_∞ criterion equals to the criterion that $X > 0$ exists to satisfy the following matrix inequation:

$$\begin{bmatrix} A^T X + XA & XE & -C^T \\ E^T X & -\gamma I & E^T \begin{bmatrix} 0 \\ I \end{bmatrix} \\ -C & \begin{bmatrix} 0 & I \end{bmatrix} E & -\gamma I \end{bmatrix} < 0 \tag{25}$$

Notice that the above matrix inequation is not a linear matrix inequation (LMI), for there is undetermined matrix in matrix A , matrix X is also undetermined. Thus the above matrix inequation cannot be solved directly. However, the method of elimination or variable substitution [12] can be adopted to convert the matrix inequation into an LMI and solve the LMI, thus obtaining the parameters A_c, B_c, C_c, D_c of the dynamic output feedback controller.

Now, the influence that the manipulator exerts on the RUAV can be effectively restrained and the stability of the RUAV platform is guaranteed. This provides the manipulator a relatively stable platform and lays the foundation for precise operation of the manipulator.

4 System Simulation and Validation

To verify the effectiveness of the control method of the manipulator, a simulation of the closed-loop controller for the actuators of the manipulator was conducted and the result is shown as Figure 5. The red dashed line in the figure is the angular expectation and the blue solid line is the actual angular motion of the manipulator. The simulation result shows that the motion of the manipulator can follow the given expectation and that the control requirements are satisfied.

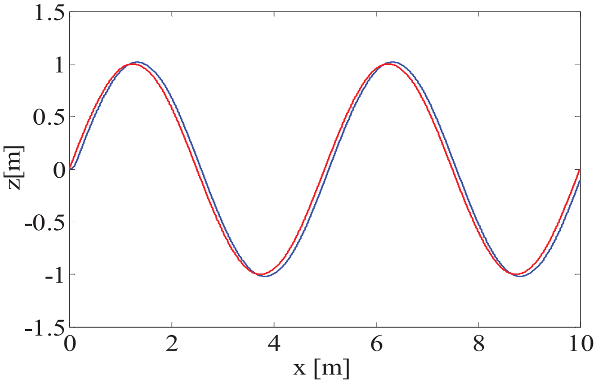

Fig.5 Response curve of manipulator control

To verify the RUAV's restraint of the disturbances caused by the manipulator, we simulated three different disturbance scenarios. In the simulation, the overall mass of the hydraulic RAM was set to be 35kg. From 10s to 20s, a force of 10N magnitude and 0.2Hz frequency was exerted along the X axis of the fuselage coordinate system to simulate the force disturbance exerted on the RUAV's fuselage along X axis which is caused by the manipulator. From 30s to 40s, a force of 10N magnitude and 0.2 Hz frequency was exerted along Y axis. From 50s to 60s, a moment of 5Nm magnitude and 0.2Hz frequency was exerted along X axis. Figure 6 shows how disturbances of different magnitudes affect the stability of the RAM system.

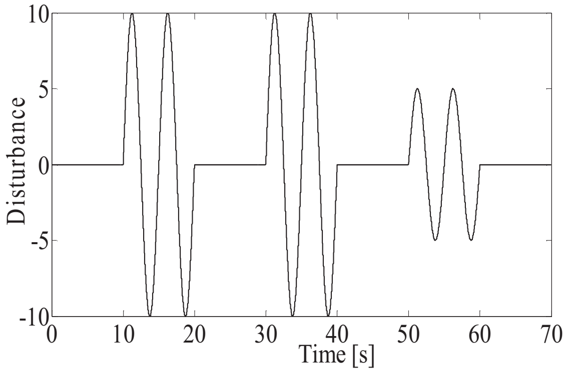

(a) Disturbance inputs

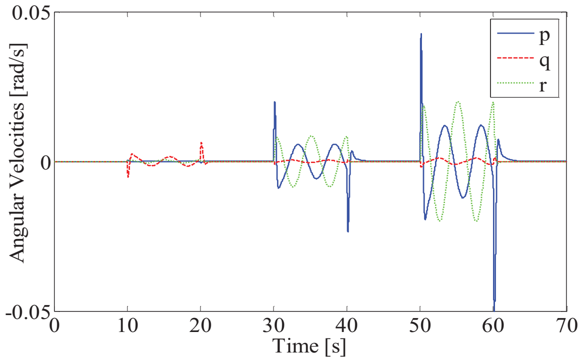

(b) Corresponding angular velocities

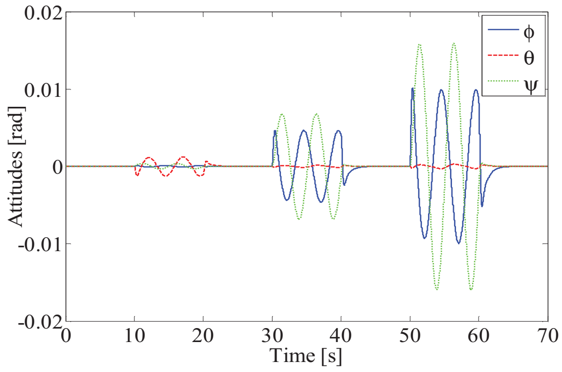

(c) Corresponding attitudes

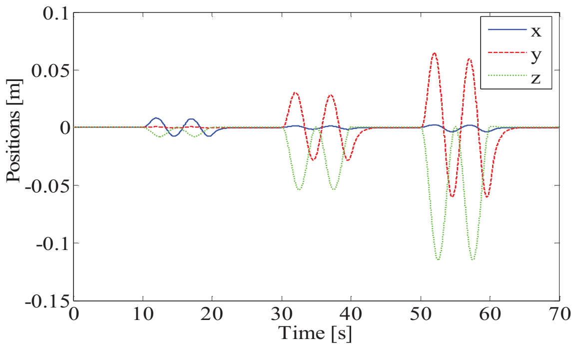

(d) Corresponding positions

Figure 6 RAM's restraint of disturbances from the manipulator

According to the simulation results shown in Figure 6, the H_∞ robust control proposed by this paper performs very well in restraining force disturbance that the manipulator exerts on the RUAV, where attitude fluctuation is smaller than 0.6 degree, position fluctuation is smaller than 0.05m. Yet, with respect to moment disturbance, the controller's performance is relatively worse. Where attitude fluctuation is smaller than 1 degree, position fluctuation is smaller than 0.1m.

Based on the model of hydraulic manipulator, model and control method of RUAV, a comprehensive simulation validation of the hydraulic RAM system had been conducted. In order to verify the scissors (end-effector) motion when the manipulator moves in the hovering mode of RAM, the manipulator's joints are set to rotate slowly in a certain range and the trajectory of the scissors was traced. Figure 7 shows the simulation result. Red dotted line in Figure 7 is the expected trajectory and the blue solid line is the trajectory of the scissors of the RAM's hydraulic manipulator. From the result of the simulation, it is verified that the RAM's shaking influence on the trajectory of the scissors which is caused by the motion of the manipulator is well restrained by the control method this paper proposed. Therefore the effectiveness of the modeling and control method proposed by this paper has been verified.

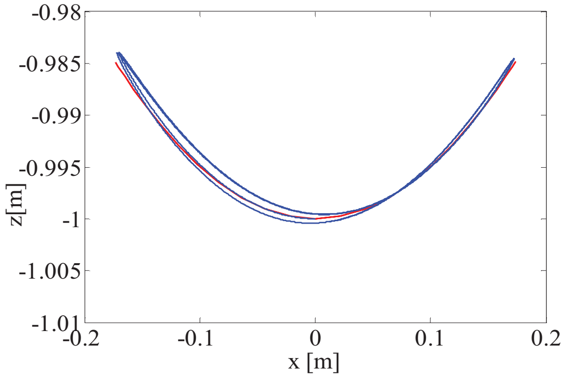

Fig.7 Trajectory simulation of scissors

5 Conclusion

The dynamics model of the hydraulic RAM (Rotorcraft Aerial Manipulator) has been established and analyzed. The corresponding controllers have been designed. An LQR controller was utilized to control the manipulator, and its effectiveness has been validated through simulation. The disturbance caused by the motion of the manipulator is restrained by a robust controller. The robustness of the robust controller has been verified through simulations using different disturbances. Under stable hovering condition, the effectiveness of the manipulator's operation is guaranteed by these characteristics of the designed controller.

In the future, a physical test simulation platform will be constructed and the aforementioned control strategies' actual performance will be examined so that the manipulator can be installed on actual RUAVs.

REFERENCES

[1] Paul E. I. Pounds, Daniel R. Bersak, Aaron M. Dollar, Grasping From the Air—Hovering Capture and Load Stability, IEEE International Conference on Robotics and Automation, 2491-2498, 2011.

[2] DLR and F. H. K. Kondak, M. Schwarzbach, M. Laiacker, D. Sommer, M. Bejar and A. Ollero, Aerial manipulation robot composed of an autonomous helicopter and a 7 degrees of freedom industrial manipulator, International Conference on Robotics and Automation, 2107-2112, 2014.

[3] J. L. Scholten, M. Fumagalli, S. Stramigioli, R. Carloni, Interaction control of an UAV endowed with a manipulator, International Conference on Robotics and Automation, 4910-4915, 2013.

[4] S. Kim, S. Choi, H. J. Kim, Aerial manipulation using a quadrotor with a two DOF robotic arm, International Conference on Intelligent Robots and Systems, 4990-4995, 2013.

[5] Xilun Ding, Yushu Yu, Dynamic analysis, optimal planning and composite control for aerial arm-operating with a

multi-propeller multifunction aerial robot, International Conference on Mechatronics and Automation, 420-427, 2013.

[6] Daqing Zhang, Qinghua He, Xuan Wu, Yunlong Zhang, Adaptive control of hydraulic excavator manipulator, International Conference on Mechatronics and Automation, 1835-1839, 2012.

[7] Tao Cheng, Track Programming and Controlling of Hydraulic Excavator, Northeastern University, 2007.

[8] Dalei Song, Juntong Qi, Lei Dai, Jianda Han, Guangjun Liu, Modeling a small-size unmanned helicopter using optimal estimation in the frequency domain, International Journal of Intelligent Systems Technologies and Applications, 8(1-4): 70-85, 2010.

[9] G. Cai, B. Chen, T. Lee, Unmanned Rotorcraft System, Springer, London, 2011.

[10] H. Shim, Hierarchical flight control system synthesis for rotorcraft-based unmanned aerial vehicles, Berkeley: University of California, 2000.

[11] P. Gahinet, P. Apkarian, A linear matrix inequality approach to H∞ control, International Journal of Robust and Nonlinear Control, Vol.5, No.4, 421-448, 1994.

[12] Yu Li, Robust control: linear matrix inequality approach. Tsinghua University Press, Beijing, 2002.